

Continuum deposition of hot dimers in one dimension

Daniel H. Linares and Victor D. Pereyra*

Department of Physics, Universidad Nacional de San Luis, Chacabuco y Pedernera, 5700 San Luis, Argentina

(Received 8 November 1995)

We study the one-dimensional hot dimer adsorption (HDA) process in the continuum. Hot dimers are molecules that dissociate instantaneously after adsorption and the resulting monomers undergo a ballistic flight up to a distance R from the deposition place. We analyze the kinetics and jamming via rate equations for the gap density distribution in the special case $R = \sigma$ (the radius of the dimer), and by means of Monte Carlo simulation for general R . The jamming density reveals an interesting dependence on the dissociative separation distance, R , where discontinuities appear for $R = \sigma, 2\sigma, 3\sigma, \dots, n\sigma$ with $n = \text{integer}$.

[S1063-651X(96)09806-6]

PACS number(s): 68.10.Jy, 82.65.-i, 02.50.-r

I. INTRODUCTION

The deposition (or adsorption) of particles on solid surfaces is a subject of considerable practical importance. In many experiments on adhesion of colloidal particles and proteins on solid substrates, the relaxation time scales are much longer than the times of the formation of the deposit. A well known example of an irreversible monolayer deposition process is the random sequential adsorption (RSA). This process is well described in the literature and has been investigated extensively in recent years [1–7].

On the other hand, recent scanning tunneling microscopy (STM) observations [8,9] of adsorption of O_2 on Al(111) have shown that, under certain conditions, oxygen molecules striking the metal surface not only dissociate instantaneously upon adsorption, but dissipate part of their excess energy in degrees of freedom parallel to the surface. As a consequence, the resulting monomers fly apart up to a distance R before being immobily adsorbed. The experiment has shown that for a temperature $T = 300$ K, the traveling distance R is, on the average, approximately 40 Å for each monomer.

This interesting process has been described by using the random sequential adsorption model [10–19]. Monte Carlo simulations have been performed to analyze the one- and two-dimensional (2D) hot dimer adsorption [10,11] and the results show that both the kinetics and the saturation state are strongly dependent on R . The analytical treatment of this dissociative adsorption process has been done in 1D [12,13].

Numerical simulation has shown that the hot dimer mechanism considerably enhances the rate of CO_2 production in the catalyzed oxidation of carbon monoxide [14]. The influence of such an adsorption mechanism has also been used to analyze the critical behavior in the monomer-dimer irreversible phase transition [15].

Recently, Mendes and Stinchcombe [19] presented a one-dimensional exact solution for the dissociative adsorption of dimers, allowing reaction between them. They analyzed the

annihilation ($A + A \rightarrow 0$) and the coalescence ($A + A \rightarrow A$) reactions of “hot” species.

Motivated by this vivid interest in the study of this finding, it is instructive to extend the analysis of the hot dimer adsorption to the continuum deposition. A previous study of the continuum deposition has been introduced in Ref. [13], however the result is restricted only to very large values of R ($R \rightarrow \infty$).

The analysis of the continuum deposition for finite values of R is not straightforward, because of the infinite hierarchies of coupled integro-differential equation for the gaps distribution density.

In this work we study, by means of the Monte Carlo simulation and (under certain conditions) an analytical approach, the hot dimers adsorption in the continuum for finite values of R .

The outline of the rest of the paper is as follows. First, we describe the model and the general equation that governs the kinetics of the process. In this section we obtain, as an example, the set of rate equations for the special case of $R = \sigma$ and their numerical solution. After that, the Monte Carlo simulation scheme is introduced and the continuum limit approximation is discussed. Finally we present the conclusions.

II. THE MODEL

As we described in Ref. [12], the adsorption of hot dimers is a dissociative adsorption process determined by two well definite steps: (a) the deposition of the dimer in at least two empty sites, and (b) after each successful deposition attempt the dimer breaks up “instantaneously” in two monomers that fly up to certain fixed distance R (in term of the lattice constant). If during the flight one monomer hits another adparticle or cluster of particles that is already at rest, the flying monomer is frozen at the collision point (site).

Based upon this particular dissociative adsorption process, we can extend the model for the adsorption in the continuum.

Our model considers the deposition of hot dimers in a one-dimensional infinite line lattice with periodic boundary condition. The length covered by the dimer is taken equal to

* Author to whom correspondence should be addressed.

2σ , where σ is the length covered by one monomer. The dimers arrive randomly at the line at a rate w per unit time per unit length. If an incoming dimer is blocked by an adsorbed adparticle, it is removed, otherwise the deposition is successful. After deposition in a free region, the dimer breaks up instantaneously and each remaining part flies apart up to a certain distance R . If during the flight one monomer hits another adparticle that is already at rest on the surface, the flying monomer is frozen at the collision point. The deposition mechanism seems to be, in some aspect, similar to the deposition of rolling spheres on the line; such a process has been analyzed by Viot *et al.* [20]. However, the similarity is restricted to the fact that, in both cases, particles move instantaneously from the original landing point to the definitive deposition or adsorption place.

The kinetics of the HDA process is monitored following the time evolution of $\bar{G}_R(\bar{l}, t) d\bar{l}$, which represents the number density of gaps with length between \bar{l} and $\bar{l} + d\bar{l}$ at time t , for a given value of R . The number density of gaps per unit length is given by

$$n_R(t) = \int_0^\infty G_R(l, t) dl, \quad (1)$$

where, for convenience, we have introduced the dimensionless variables $t = \sigma w \bar{t}$, $l = \bar{l} \sigma$, and $G_R = \sigma \bar{G}_R$.

The density is also related to the fraction of the covered surface, i.e., the fraction of the line covered by the particles,

$$\rho_R(t) = 1 - \int_0^\infty l G_R(l, t) dl. \quad (2)$$

Due to the nature of the deposition process, that is, one monomer can hit another adparticle or cluster of adparticles and each gap does not correspond necessarily to one particle, we have $\rho_R(t) \neq n_R(t)$.

The rate equations of the gap distribution function can be written in a closed form by considering all the ways in which intervals may be created or destroyed during the hot dimer deposition process. For a given interval (gap) of length $l > 2\sigma$, the available length for the insertion (deposition) of a dimer is the inner interval of length $l - 2\sigma$ (step a), see Fig. 1(a). A number of different situations appear due to the fact that, after deposition, each monomer flies up to a fixed distance R (step b). As a consequence, the ways of creation and destruction of the gaps depend on the relation between R and the length of a given gap l , see Fig. 1(b). For large values of R ($R \rightarrow \infty$), the destruction of a gap of length $l > 2\sigma$, is followed by the creation of a unique inner gap of length $l - 2\sigma$, independent of the value of l and the place of the deposition of the dimer. In the other extreme, the case $R = 0$, we have the classical ‘‘car parking problem’’ [21], where the jamming density is well known $\rho_0(\infty) = 0.747598$. For finite values of $R \neq 0$, the destruction of a given gap of length $l > 2\sigma$, can be followed by the creation of one inner gap limited by the monomers and up to two more gaps, between the monomers and the particles or clusters of particles which are already at rest. In the last case, the number of ways of creation of the gaps with length $l' < l$ depend on the relation between l and R and the place of the deposition of the dimer. On the other hand, given that

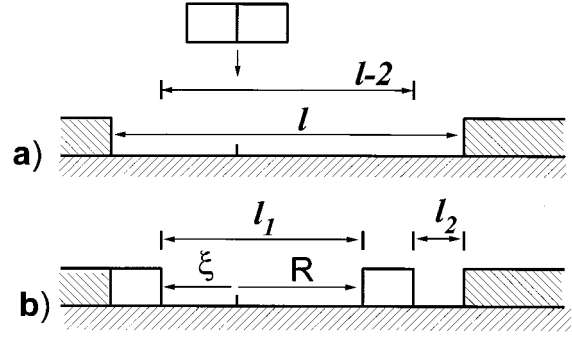


FIG. 1. Illustration of the deposition process. (a) The incoming dimer of size 2σ (here $\sigma = 1$) arrives at the line and its center is deposited in the $(l - 2)$ possible place. (b) The destruction of a given gap of length $l > 2$ can be followed by the creation of one inner gap of length $0 < l_1 \leq 2R$ limited by the monomers and up to two more gaps (in the figure we show only one) with length $0 \leq l_2$. Note that one of the monomers in the figure travels a distance $\xi < R$.

the probability of an incoming dimer to fall in a gap of length $l \leq 2\sigma$ is strictly zero, such gaps are always created in the HDA process. However, we have to distinguish three different possibilities: (i) gaps of length $l = 2\sigma$, (ii) gaps of length between $\sigma < l < 2\sigma$, and, finally, (iii) gaps of length $l < \sigma$. In the case (i) the number of gaps of length 2σ is highly increased for small integer values of the parameter R/σ . The reason for such an effect will be discussed below.

According to the definition of our model, the kinetics of the process is given by the time evolution of $G_R(l, t)$. To illustrate the method, we present in the rest of the section the derivation of the rate equations and their numerical solution for one particular case, $R = \sigma$. To simplify the treatment, we consider, in what follows, that the radius of the dimer takes the value $\sigma = 1$. From the argument described below, we obtain the following set of coupled equations:

$$\frac{dG_\sigma(l, t)}{dt} = -(l - 2)G_\sigma(l, t) + 2 \int_{l+3}^\infty G_\sigma(l', t) dl' \quad (l > 2), \quad (3a)$$

$$\frac{dG_\sigma(l, t)}{dt} = \int_4^\infty (l' - 4)G_\sigma(l', t) dl' \quad (l = 2), \quad (3b)$$

$$\begin{aligned} \frac{dG_\sigma(l, t)}{dt} = & (2 - l)G_\sigma(l + 2, t) + 2 \int_{l+2}^{l+3} G_\sigma(l', t) dl' \\ & + 4 \int_{l+3}^\infty G_\sigma(l', t) dl' \quad (1 < l < 2), \end{aligned} \quad (3c)$$

$$\frac{dG_\sigma(l, t)}{dt} = lG_\sigma(l + 2, t) + 2 \int_{l+3}^\infty G_\sigma(l', t) dl' \quad (0 < l < 1). \quad (3d)$$

Equation (3a) describes the time evolution of the gap distribution function for gaps with length $l > 2$. These gaps are destroyed by the deposition of a dimer in the $l - 2$ possible inner place. The creation of such gaps is described by the second term in the right-hand side of the equation. The factor

of 2 in the creation term reflects the two possibilities of breaking a larger interval by inserting a dimer.

Equation (3b) represents the evolution of the gap distribution function, for a gap of size exactly 2. Due to the fact that the flight distance of each monomer is between 0 and $R(R=1)$, the gaps of size exactly 2 are always created in the process by the gaps with length l' between 4 and ∞ , provided that the incoming dimer falls in an inner interval, which is located at a distance 2 from one of the borders of this gap. There are $l'-4$ possibilities to fall in such an interval. It is clear that the probability to destroy the gaps of length exactly 2 is strictly 0.

Equation (3c) considers the time evolution of the gaps with length between $(1 < l < 2)$. The first term on the right-hand side of the equation takes into account the creation of these gaps due to the deposition of the incoming dimer in a gap with length $l+2$, provided that the center of the dimer falls in an interval of length $2-l$ located at a distance of 1 of the border. The next term is due to the contribution of the gaps with length between $l+2$ and $l+3$; the factor of 2 reflects the two possibilities that the dimer falls in this gap. The last term of this equation has a factor of 4, which denotes the four deposition possibilities in gaps with length bigger than $l+3$.

Finally, we have the evolution of the gaps smaller than 1. In this case the contribution of the gaps with length $l+2$ is reflected in the first term of the right-hand side of Eq. (3d), where the factor l represents the probability that the incoming dimer falls in these gaps. The following term is given by the contribution of the gaps with length bigger than $l+3$.

In order to solve the previous set of coupled integro-differential equations, we use the standard procedure developed in Ref. [1]. The solution can be obtained by considering first the interval larger than 2. Inserting the following ansatz for $G_\sigma(l, t)$ in Eq. (3a),

$$G_\sigma(l, t) = F(t)t^2 e^{-(l-2)t} \quad (l > 2), \quad (4)$$

and replacing the expression of $G_\sigma(l, t)$ in Eqs. (3b), (3c), and (3d), we can obtain the following expression for the complete set of equations:

$$G_\sigma(l, t) = \int_0^t F(\mu) e^{-2\mu} d\mu \quad (l=2), \quad (5a)$$

$$G_\sigma(l, t) = \int_0^t \mu F(\mu) e^{-l\mu} [2(1 + \mu + e^{-\mu}) - l\mu] d\mu \quad (1 < l < 2), \quad (5b)$$

$$G_\sigma(l, t) = \int_0^t \mu e^{-l\mu} (2e^{-\mu} + l\mu) d\mu \quad (0 < l < 1), \quad (5c)$$

where $F(t)$ is given by

$$F(t) = e^{-2 \int_0^t [1 - e^{-3\mu}/\mu] d\mu}. \quad (6)$$

We can calculate, by using the expression of $G_\sigma(l, t)$, the corresponding fraction of the line uncovered by particles $H_i(t)$, which is independent of l , as

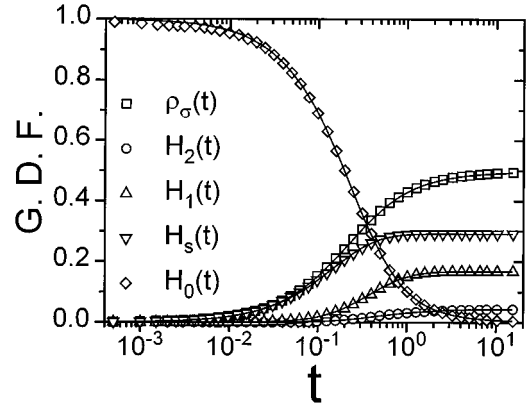


FIG. 2. Gaps distribution functions (GDF) $H_i(t)$ and density $\rho_\sigma(t)$, as a function of time for $R=\sigma$. The numerical solutions of the rate equations (line) compare with Monte Carlo simulations (symbols).

$$H_0(t) = F(t)(2t+1) \quad (l > 2), \quad (7a)$$

$$H_s(t) = 2 \int_0^t F(\mu) e^{-2\mu} d\mu \quad (l=2), \quad (7b)$$

$$H_1(t) = \int_0^t \mu F(\mu) [2(1 + \mu + e^{-\mu}) I_1(1, 2, \mu) - \mu I_2(1, 2, \mu)] d\mu \quad (1 < l < 2), \quad (7c)$$

$$H_2(t) = \int_0^t \mu F(\mu) [2e^{-\mu} I_1(0, 1, \mu) + \mu I_2(0, 1, \mu)] d\mu \quad (0 < l < 1), \quad (7d)$$

where $I_n(a, b, t)$ is defined as

$$I_n(a, b, t) = \int_a^b l^n e^{-lt} dl. \quad (8)$$

To calculate the density we use the expression given in Eq. (2). Then we have

$$\rho_\sigma(t) = 1 - [H_0(t) + H_s(t) + H_1(t) + H_2(t)]. \quad (9)$$

In Fig. 2 we show the numerical solution for the density and the fraction of the uncovered surface $H_i(t)$ as a function of time t (line) compare with the Monte Carlo simulation results (dots). The simulation procedure is described in the next section. We can observe an excellent agreement between both methods. The jamming density is obtained by solving numerically Eq. (9) for very large values of $t(t \rightarrow \infty)$; the result is $\rho_\sigma(\infty) = 1/2$.

The asymptotic approach to the saturation density is shown in Fig. 3, and we can observe that the dependence of $\rho_\sigma(\infty) - \rho_\sigma(t)$ is proportional to t^{-1} as in the classical continuum deposition [1]. We can conclude that the asymptotic behavior does not depend on the ‘‘hot’’ adsorption mechanism. In principle, the general solution could be obtained by solving the set of coupled integro-differential equations which governed the time evolution of $G_R(l, t)$, however, it is necessary to derive a different set of equations for each in-

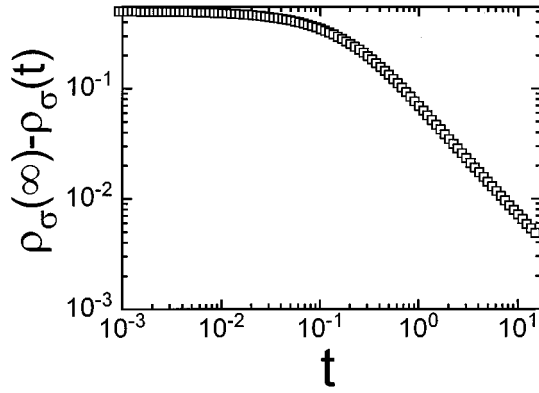


FIG. 3. Asymptotic regime approach for $R = \sigma$. The slope of the curve $\propto t^{-1}$ does not depend on the hot adsorption mechanism.

terval defined by successive integer values of R/σ . As a consequence, the treatment of the problem by solving the rate equation for larger values of R/σ becomes impractical. For this reason we have used the Monte Carlo simulations, as an alternative, to analyze the process for general R .

III. MONTE CARLO SIMULATION SCHEME

The Monte Carlo simulation of the “hot” dimer deposition in the continuum is analyzed by using the standard procedure described in Ref. [4]. For the continuum deposition of the dimer of size 2σ , on a 1D line with periodic boundary condition, it is convenient to introduce the corresponding lattice model, where the dimer is replaced by a “ $2k$ -mer.” Thus, we introduce a lattice of spacing $b = \sigma/k$, and allow deposition only at sites where the incoming particle will coincide *exactly* with the underlying lattice, covering $2kb$ units. The deposition frequency per site will be w . The deposition attempts are successful if the incoming particles do not overlap any particles already in the deposit. Each successful deposition attempt of the $2k$ -mers is followed by an instantaneous fragmentation in two parts of length kb and each of them flies up to a certain distance R , as we described above. In the limit $k \rightarrow \infty$ ($b \rightarrow 0$), we obtain the continuum deposition. In our simulation, we keep the k -mer notation as before and define the dimensionless time $t = w\sigma\bar{t}$. In the hot deposition we also observe that the jamming coverage, in the lattice, approached exponentially for large time t . On the other hand, for the continuum we have observed that in the asymptotic limit the jamming density approached as a power-law, $\propto t^{-1}$. The crossover between these two behaviors is similar to the classical RSA problem and is not analyzed in this work. An interesting feature, which is only a characteristic of the hot dimer deposition mechanism, appears in the approximation to the continuum limit ($k \rightarrow \infty$). In the filling process, the early depositions determine a strongly correlated configuration. In fact, at the beginning of the process, most of the dimers arrive at the empty line, and after fragmentation each monomer flies up to exactly a distance of R , independently of k , increasing the population of gaps by exactly $2R$. In the case of $R = kb$, the size of these gaps coincides with the size of the dimer. The probability to cover such empty gaps of exactly $2kb$ (the size of the dimer) is proportional to $\propto 1/2k$. As the value of k increases (limit to

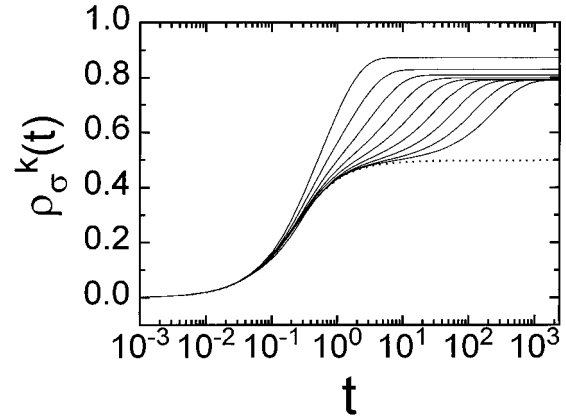


FIG. 4. Time dependence of the density for the case $R = \sigma$ and for different values of k ($k = 2, 4, 8, 16, 32, 64, 128, 256, 512$). The topmost datum is 2, and the lower data set corresponds to the decreasing k values. The dashed curve corresponds to the “off-lattice” simulation. We can clearly observe the jamming state (arrows) corresponding to $\rho_{\sigma}(\infty) = 0.5$ and $\rho_{\sigma}^k(\infty) = 0.7999$ for large values of k .

the continuum) the probability to cover the gaps diminishes, but is always finite. As a consequence, in the approach to the asymptotic limit ($t \rightarrow \infty$) there is, always, a crossover between the jamming density corresponding to the continuum $\rho_R(\infty)$ and the jamming density obtained in the limit procedure $\rho_R^k(\infty)$; see Fig. 4. We can see in Fig. 5 that for the jamming density $\rho_R^k(\infty)$, plotted vs $1/k$ for different values of R , it is possible to observe that $\rho_R^k(\infty)$ is independent of k , for large values of this parameter.

The second jamming state is produced by the lattice approximation in the limit procedure, and only for integer values of R/σ ($R \neq 0$) is the effect present. This is because only in this case is the formation of gaps of size exactly $2kb$ possible. We can conclude that this “jamming state” is a finite size effect due to the fact that in our limit procedure, for any finite value of the parameter k , we have a finite probability to cover the gap of size $2kb$, no matter how large

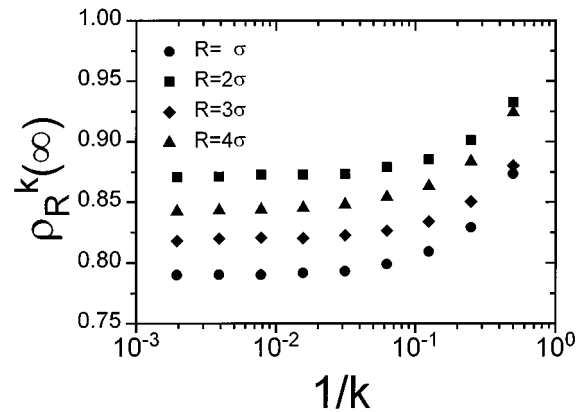


FIG. 5. Size dependence of the second jamming density $\rho_R^k(\infty)$ plotted vs $1/k$ for different values of the parameter R . We can observe that for large values of k , $\rho_R^k(\infty)$ is constant and independent of k .

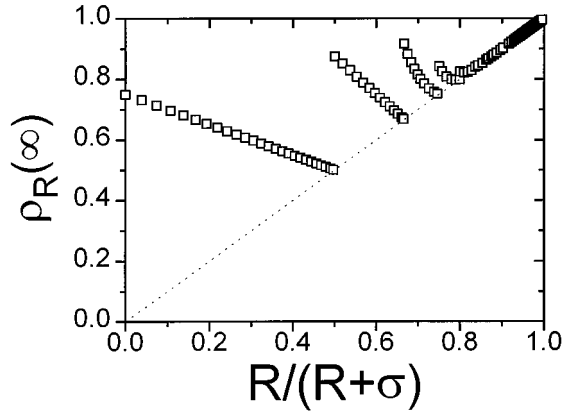


FIG. 6. Jamming density $\rho_R(\infty)$ as a function of $R/(R+\sigma)$. We can observe the finite discontinuity for $R=\sigma, 2\sigma, 3\sigma, \dots, n\sigma$ ($n = \text{integer}$). The dashed line is drawn as a guide to the eye.

the value of k is. As a consequence, we can always observe a crossover between the jamming density $\rho_R(\infty)$ corresponding to the “real” jamming state, and the jamming density $\rho_R^k(\infty)$ corresponding to the “apparent” jamming state. The crossover time or the time required by the system to reach the final state is proportional to $2k$. We can modify the rate equation in order to consider this effect by introducing Eq. (3b), the destruction of the gaps of size 2σ , provided that a dimer falls in such a gap with some finite probability. Then the equation will be modified by adding the term $-\alpha G_\sigma(t)$, where α is the probability that the incoming dimer falls in such an interval. The solution of the kinetics equations is in agreement with the simulations results provided that the probability α is equal to $1/2k$.

To avoid any size effect in our numerical experiment we have performed “off-lattice” simulation by using a large value of k ($k=2^{48}$) and the length of the lattice in the interval $L=10^5$ to 10^6 depending on the value of R in use. Our Monte Carlo time unit corresponds to L trials of deposition of dimers. The results were averaged over a number of 10^2 samples, depending on the size of the lattice. The simulations were carried out at the PARIX parallel computer system with eight nodes.

One interesting aspect of the continuum deposition of the hot dimer is the R dependence of the jamming density. In the discrete, the dependence of the jamming coverage with R is given by a power-law $|\theta_\infty(\infty) - \theta_R(\infty)| \propto R^{-x}$, where the exponent is $x \approx 0.9$ with $\theta_\infty(\infty)=1$ in one dimension and $x \approx 0.5$ with $\theta_\infty(\infty)=0.943$ in a two-dimensional square lattice [11].

In contrast to the simple power-law dependence of the jamming coverage in the discrete lattice (1D and 2D), the jamming density $\rho_R(\infty)$ for the hot dimer deposition in the continuum exhibits a very rich behavior as a function of the flight distance R . We have plotted in Fig. 6 $\rho_R(\infty)$ vs $R/R+\sigma$. We can observe that, for $R=\sigma, 2\sigma, 3\sigma, \dots, n\sigma$ with $n = \text{integer}$, the jamming density described a perfect straight line which is given by

$$\rho_R(\infty) = \frac{R}{R+\sigma} \quad \text{for } R=\sigma, 2\sigma, 3\sigma, \dots, n\sigma \quad (n=\text{integer}). \quad (10)$$

We can observe (see Fig. 6) that the limit values of the jamming density, as a function of R , are according to previous analysis. In fact, for $R=0$ we have the classical car parking model, where the jamming density is $\rho_0=0.747598$ [21] and for $R \rightarrow \infty$ the jamming density tends to 1 [12,13]. For values of the parameter R/σ between 0 and 1, the size of inner gaps created in the separation of one deposited dimer is smaller than 2σ ; for this reason such inner gaps cannot be covered in the entire process. As the value of R/σ increases, the size of the empty gaps also increases and as a consequence the jamming density diminishes monotonically between $\rho_0=0.747598$ and $\rho_\sigma=0.5$. For $R>\sigma$ the size of the inner gaps created in the deposition process is bigger than 2σ and can be filled by the incoming dimers. One of the most interesting features that we can observe in the curve is given by the finite discontinuities of $\rho_R(\infty)$, near the integer values of R/σ . The explanation of such discontinuity is based on the same argument discussed before; the probability to fill a gap with size exactly 2σ is 0. As we increase the values of R to $R+dR$, the gaps of $2R$, which were generated in the earliest deposition, will be filled with some finite probability and the jamming density will be higher than those corresponding to the integer R/σ . As a consequence, the value of the jamming density is higher at the right of one integer value of R/σ and decreases monotonically until the next integer R/σ . At values of $R/\sigma > 5$ the effect becomes so small that the discontinuities cannot be detected by simulations. This is due to the fact that the populations of gaps with size $2R$ diminish as the value of R increase.

IV. CONCLUSION

In this paper, we have presented a model for the deposition of hot dimers in the continuum. By means of numerical simulation and an analytical approach we have studied the so-called “hot” dimers adsorption in the continuum for finite flight distance R . We can develop the kinetic equations for the gaps distribution function for a particular value of the parameter R ($R=\sigma$). The numerical solution of the rate equations is in good agreement with the Monte Carlo simulations results. An apparent jamming state emerges for the integer values of the parameter R/σ as a consequence of the finite size effect in the adsorption mechanism. This effect is only present in the continuum limit procedure and is due to the presence of gaps of exactly 2σ size. Those gaps have been covered by the incoming dimers with a probability proportional to the size of the discrete dimers $\alpha=1/2k$. In the limit $k \rightarrow \infty$ these gaps remain uncovered given the real jamming density $\rho_R(\infty)$. The jamming state, as in the discrete, depend on the parameter R , however one of the most interesting features, which differentiates between the continuum deposition and the RSA of hot dimers in the lattice, is the piecewise profile that characterizes the jamming density as a function of the flight distance R . The rich structure observed in the profile contains finite discontinuities near the integer values of $R=\sigma, 2\sigma, 3\sigma, \dots, n\sigma$ with $n = \text{integer}$, which are explained by the fact that the probability to cover the gaps of size $2R$ by the incoming dimers is strictly 0. For such values of the parameter R a simple law is obeyed by the jamming density $\rho_R(\infty)=R/(R+\sigma)$.

ACKNOWLEDGMENTS

This work is partially supported by the Consejo Nacional de Investigaciones Científicas y Técnicas and Fundación Antorchas (Argentina). The European Economic Community,

Project ITDC-240, is greatly acknowledged for the provision of valuable equipment. The authors would like to acknowledge stimulating discussions with Professor E.V Albano and Dr. R.A. Monetti. One of the authors (V.P.) would like to thank Dr. E. Duering for suggesting the problem.

-
- [1] J.W. Evans, *Rev. Mod. Phys.* **65**, 1281 (1993).
[2] M.C. Bartelt and V. Privman, *Int. Mod. Phys. B* **5**, 2883 (1991).
[3] J.J. Gonzalez, P.C. Hemmer, and J.S. Hoye, *Chem. Phys.* **3**, 228 (1974).
[4] V. Privman, J.-S. Wang, and P. Nielaba, *Phys. Rev. B* **43**, 3366 (1991).
[5] J.W. Evans and R.S. Nord, *J. Stat. Phys.* **38**, 681 (1985).
[6] J. Talbot, G. Tarjus, and P. Schaaf, *Phys. Rev. A* **40**, 4808 (1989).
[7] P. Schaaf and J. Talbot, *Phys. Rev. Lett.* **62**, 175 (1989).
[8] H. Brune, J. Wintterlin, R.J. Behm, and G. Ertl, *Phys. Rev. Lett.* **68**, 624 (1992).
[9] H. Brune, J. Wintterlin, J. Trost, G. Ertl, J. Wiechers, and R. J. Behm, *J. Chem. Phys.* **99**, 2128 (1993).
[10] V.D. Pereyra and E. Albano, *J. Phys. A* **26**, 4175 (1993).
[11] E. Albano and V.D. Pereyra, *J. Chem. Phys.* **98**, 10 044 (1993).
[12] V.D. Pereyra, E. Albano, and E. Duering, *Phys. Rev. E* **48**, R3229 (1993).
[13] V. Privman, *Europhys. Lett.* **23**, 341 (1993).
[14] V.D. Pereyra and E. Albano, *Appl. Phys. A* **57**, 291 (1993).
[15] E. Albano and V.D. Pereyra, *J. Phys. A* **27**, 7763 (1994).
[16] R.A. Monetti, E.V. Albano, and V. Pereyra, *J. Chem. Phys.* **100**, 5378 (1994).
[17] R.A. Monetti and E. V. Albano, *Physica A* **206**, 289 (1994).
[18] R.A. Monetti and E. V. Albano, *Physica A* **214**, 475 (1995).
[19] J.F.F. Mendes and R. B. Stinchcombe, *Europhys. Lett.* **27**, 227 (1994).
[20] P. Viot, G. Tarjus, and J. Talbot, *Phys. Rev. E* **48**, 480 (1993).
[21] A. Renyi, *Sel. Trans. Math. Stat. Prob.* **4**, 205 (1963).